

Performance Prediction in Long Operation for Magnetic-Layer-type Hall Thrusters

IEPC-2009-140

*Presented at the 31st International Electric Propulsion Conference,
University of Michigan • Ann Arbor, Michigan • USA
September 20 – 24, 2009*

Hirokazu Tahara^{*}, Tsuyoshi Fujita[†] and Yudai Shimizu[‡]
Osaka Institute of Technology, Asahi-Ku, Osaka, 535-8585, Japan

Abstract: The magnetic-layer-type Hall thruster THT-VI, which has the same channel configuration as Russian SPT-100 Hall thruster, was operated. This thruster is provided with a trim coil to alter magnetic topology in the acceleration channel. The performance was enhanced with the trim coil in some operational conditions. Both the discharge current and the thrust were affected by small changes of the channel shape. Accordingly, performance changes in long operations were predicted by this scheme. The experimental results showed that the performance is gradually deteriorated during 0-300 hour predicted operation. Furthermore, numerical simulation was carried out by using hybrid Particle-In-Cell method, and its result was compared with the experimental one. The calculated performance quantitatively agreed with the measured one. The calculated 2000 h operation showed that the acceleration channel was intensively shaved near the downstream exit by spattering enhanced with highly accelerated ions. The inner channel wall was relatively severe compared with the outer channel wall. Also, the calculated dependence of channel material on performance showed that the BNAIN channel with a high secondary electron emission coefficient has the highest performance.

Nomenclature

d	= length
E	= electron charge
K	= Boltzmann constant
p	= pressure
r	= radial direction
s	= small area
T	= time
u	= velocity
E	= electric field or energy
I	= current
S_{wall}	= electron energy loss on channel wall
T	= temperature
T_{sec}	= secondary electron emission temperature
ϵ_{eff}	= secondary electron emission coefficient
	= length
ν_{ion}	= ionization collision frequency
	= potential

^{*} Professor, Department of Mechanical Engineering, and tahara@med.oit.ac.jp.

[†] Graduate Student, and Department of Mechanical Engineering.

[‡] Graduate Student, and Department of Mechanical Engineering.

Subscripts

O	=	initial
a	=	anode
E	=	electron
I	=	ion or ionization
L	=	final
w	=	wall

I. Introduction

Hall thrusters, familiarly known as Stationary Plasma Thrusters (SPTs), are plasma accelerators widely used for satellite station keeping and deep space exploration.¹ In years, leading SPT research and development efforts have been undertaken in Russia, US, Europe, and Japan.²⁻⁵

The Hall thruster has an anode-cathode system with a dielectric annular channel where the propellant ionization and acceleration processes occur. This thruster works using a perpendicular electric and magnetic field configuration. The generated electric field subsequently accelerates the produced ions to a high exhaust velocity (~20 km/s). Because of high exhaust velocity, SPTs consume much less propellant than conventional chemical propulsion devices. A magnetic circuit generates an axisymmetric and quasiradial magnetic field in the acceleration channel. The operating feature and performance of the Hall thruster are very sensitive to the magnetic field topology. In a previous study, it was known that good performance was obtained with magnitude maximum of magnetic field in the exit plane and minimum in the anode region.⁶ To adjust the magnetic field gradient in the exhaust region and to reduce the magnetic field magnitude in the anode region, a magnetic screen surrounding the acceleration channel is usually equipped. Enhancement of thruster performance by the magnetic screen has already confirmed⁷. This parts, however, makes thruster's structure heavier and more complex, which is negative in the viewpoint of commercial viability.

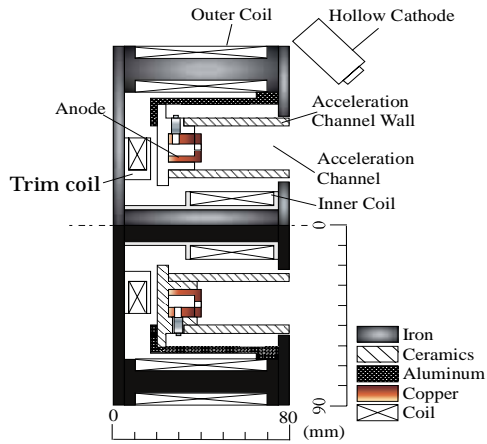
Our research members fabricated THT-VI thruster which has an auxiliary coil (a trim coil) positioned behind the anode to alter the magnetic field topology and create a zone of lower magnetic field inside the channel instead of a magnetic screen. The axial gradient of magnetic field $\partial_z B_r$ can be changed depending on the direction of the coil current. A negative current reduces the magnetic field near the anode, and increases the value of $\partial_z B_r$.

In this study, performance characteristics with the trim coil are investigated. Discharge current and thrust are measured with varying magnetic field topology at a constant discharge voltage, and then thrust efficiency is estimated. Furthermore, time variations of performance are studied with special channel geometries artificially changed considering long operations. This study will lead to estimation of lifetime of Hall thrusters. Numerical calculation is carried out by means of hybrid Particle-In-Cell (PIC) method including lots of physical effects of secondary electron emission, sheath creation and ion sputtering etc. on the acceleration channel. The experimental results are compared with the calculated ones. The dependence of channel material species on performance and plasma feature is also calculated.

II. Experimental apparatus

Figure 1 shows the schematic of the 1kw laboratory model THT-VI thruster is classified as the magnetic layer or stationary plasma thrusters. The thruster has a discharge channel with an outer diameter of 100 mm and an inner diameter of 56 mm, i.e., with 22mm in width, and the channel length is 40mm. The channel dimensions are the same as those of SPT100. The discharge channel wall is made of Boron Nitride (BN). In THT-VI thruster, the circuit which applies the magnetic field B_r in the channel consists of an inner coil, six outer coils and a trim coil. We always applied the negative current to a trim coil three times as much as inner and outer coils, for the reason that the ratio is optimum condition for performance. Inner and outer coils are connected in series, and a trim coil is independent.

Figure 2 shows the measured axial distribution of magnetic field strength on the channel median of THT-VI thruster for cases with and without a trim coil. It was measured by a magnetic probe. Figure 3 shows the calculated magnetic field lines at each case. The axial gradient of magnetic field is changed, and the region of large magnetic field, as shown in Figure.2, is pushed toward the exit when a trim coil is used. In the anode region, the magnetic field is lower. First, we operated the thruster without the use of a trim coil, and then energized a trim coil. We made a comparison between with and without the use of a trim coil in thrust, discharge current and thrust efficiency.



(a) Cross-sectional view.

(b) Photo.

Figure 1. Schematic of THT-VI Hall thruster.

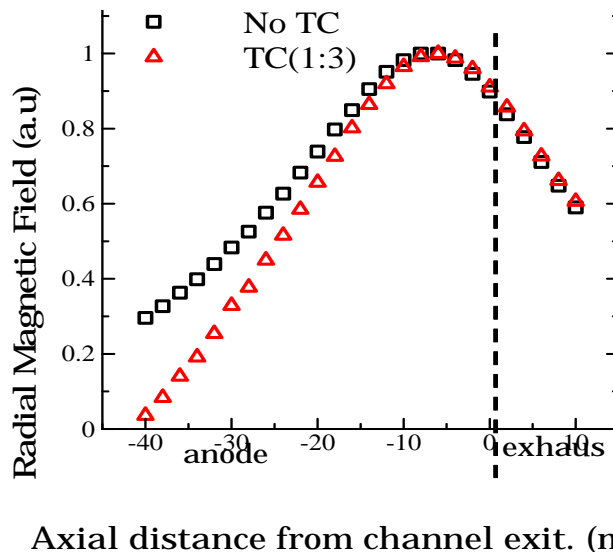
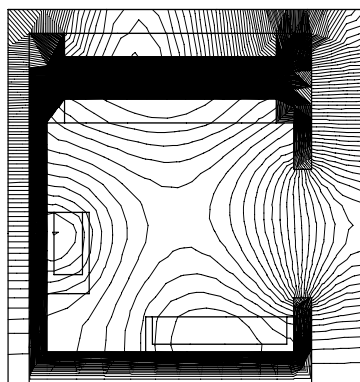
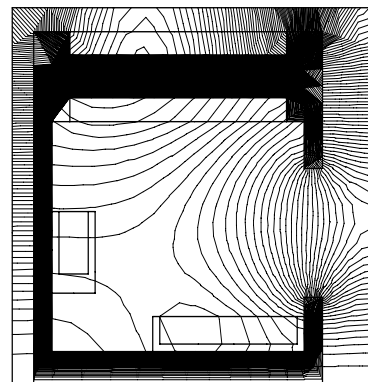


Figure 2. Axial distributions of radial magnetic field strength in acceleration channel with and without trim coil.



(a) Without trim coil.



(b) With trim coil.

Figure 3. Calculated magnetic field lines in THT-VI thruster.

A hollow cathode (Iontech HCN-252) is used as a cathode. Table 1 shows an operating condition of the present experiment. The operating condition is varied with discharge voltages of 200-400 V. Xenon is used as the propellant. The mass flow rate is 2 mg/s.

The experimental facility is shown in Figure.4. The thruster is operated in a water-cooled stainless steel vacuum chamber that is 1.2 m in diameter and 2.25 m in length. The chamber is equipped with two compound turbo molecular pumps that have a pumping speed of 10000 l/s on xenon, several DC power supplies, and a thrust measurement system. The vacuum chamber pressure is kept about 3.0×10^{-2} Pa under operation. A clean and high vacuum environment can be created by using the oil-free turbo molecular pump system.

Figure 5 shows the schematic view of the thrust measurement system.²⁻⁵ A pendulum method is used in order to measure thrusts. The thruster is mounted on a thrust stand suspended with an aluminum bar, and the displacement of the thruster is detected by an eddy-current-type gap sensor. It has a high sensitivity and good linearity. Thrust calibration is conducted with a weight and knife-edge arrangement, which can apply a known force to the thruster under vacuum condition.

Discharge current oscillation is measured with a current probe (Iwatsu: SS-250), and is observed with a high speed camera (Photron: FASTCAM APX RS).

Table 1. Operational conditions for THT-VI thruster

Discharge voltage	200 ~ 400V	
Propellant	Xenon	
Mass flow rate	THT-	2.0mg/s
	Hollow cathode	0.1mg/s
Coil current	Inner, outer coil	0.2 ~ 0.5A
	Trim coil	0.6 ~ 1.5A
Coil current ratio	Inner, outer : trim	1:3
B_{max}	100 ~ 130 Gauss	
Back-pressure	3.0×10^{-2} Pa	

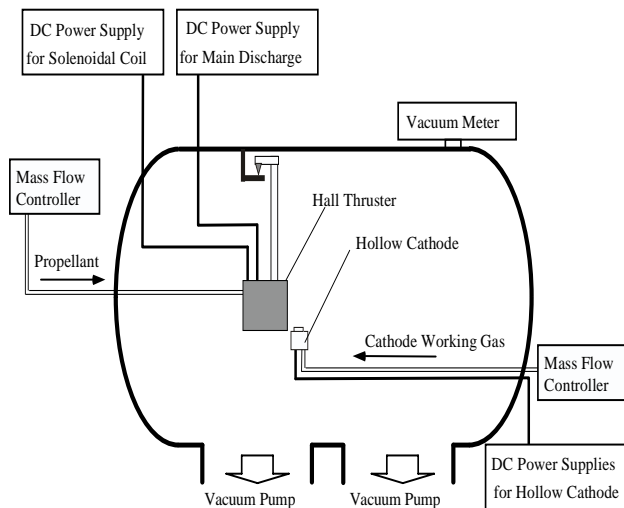


Figure 4. Experimental facility for Hall thruster.

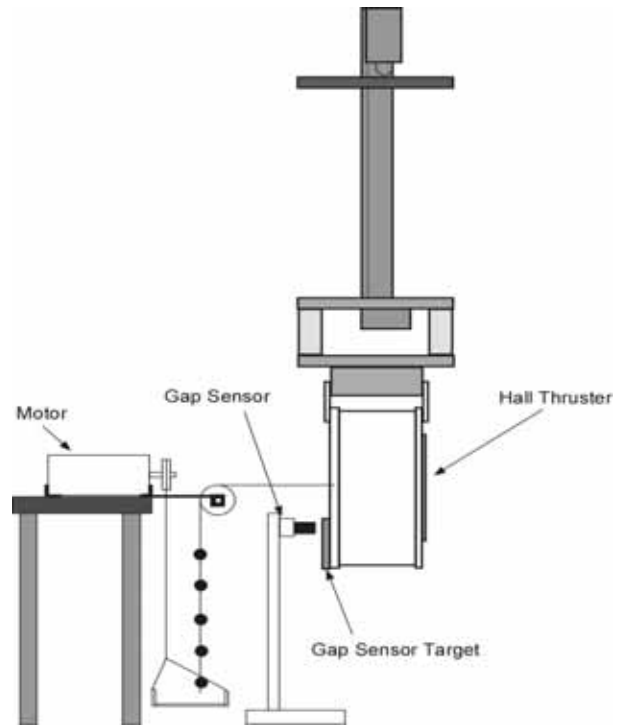


Figure 5. Thrust measurement system for Hall Thruster.

Ions accelerated inside the acceleration channel are bombarding near the downstream exit of the channel, resulting in changing geometry of the BN channel by ion sputtering. The acceleration channel exit of THT-VI thruster is shaved as shown in Figure.6 in order to predict performance characteristics after several hundreds hour operation. The amounts of shaving mass and sloop were roughly determined by previous endurance tests and numerical simulations with SPT-100 Hall thruster in Refs. 8 and 9. In this study, the estimation times are 0, 100, 200 and 300 hour.

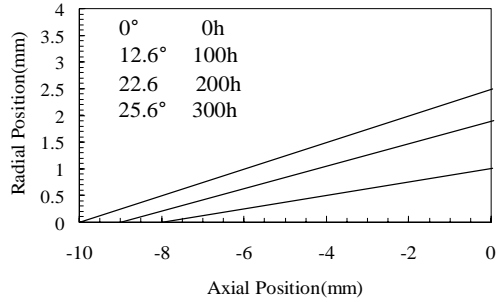


Figure 6. Shaving shapes of acceleration channel walls and their predicted operational times for THT-VI thruster.

III. Numerical Simulation

Hall thruster discharge plasma is numerically simulated by hybrid PIC method. The axisymmetric two-dimensional code is developed to predict performance characteristics and finally to predict lifetime.

A. Calculation domain

Figure.7 and Table 2 show the calculation domain for THT-VI thruster. All dimensions are the same as THT-VI thruster. The length is 40 mm in the acceleration channel and 10 mm outside the channel. The other calculation domain including the BN acceleration channel insulators, as shown in Figure.8, is also used when predicting the change of acceleration channel geometry by ion sputtering in long operations.

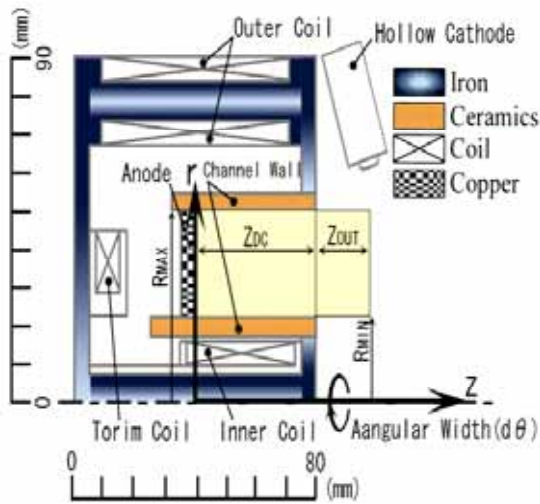


Figure 7. Calculation domain for initial performance prediction.

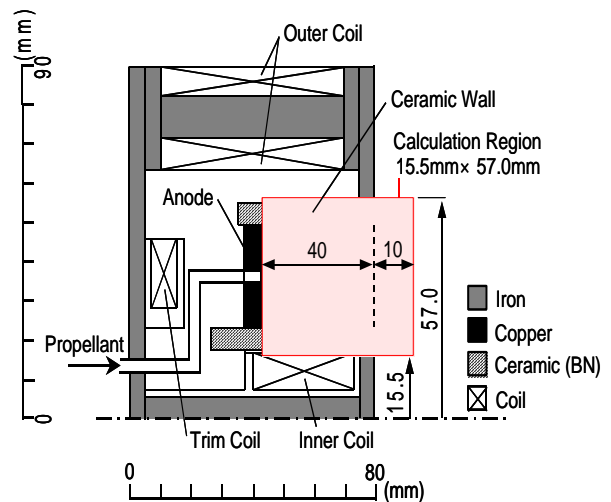


Figure 8. Calculation domain including channel insulators for long-time performance

Table 2. Calculation domain details.

Calculation Region	27.5 × 50 [mm ²]
R _{MAX}	50.0 [mm]
R _{MIN}	22.5 [mm]
L _{DC}	40.0 [mm]
L _{OUT}	10.0 [mm]
dθ	π / 180 [rad]

B. Calculation model and procedure

A hybrid PIC code is developed to simulate physical phenomena inside Hall thrusters. The ion and the electron are treated as particle and fluid, respectively, in this calculation. The main governing equations are follows.

Conservation of current:

$$I_a = -2\pi e \int_0^l n_i u_{i,\hat{n}} r ds + 2\pi e \int_0^l n_e u_{e,\hat{n}} r ds \quad (1)$$

Ohm's law perpendicular to magnetic field:

$$u_{e,\hat{n}} = \mu_{e,\perp} \left(\frac{\partial \phi^*}{\partial \hat{n}} + \frac{k}{e} (\ln(n_e) - 1) \frac{\partial p_e}{\partial \hat{n}} \right) \quad (2)$$

Potential on magnetic field line:

$$\phi = \phi^*(\lambda) + \frac{kT_e}{e} \ln(n_e) \quad (3)$$

Conservation of electron energy:

$$\frac{\partial}{\partial t} \left(\frac{3}{2} n_e kT_e \right) + \nabla \cdot \left(\frac{5}{2} n_e kT_e u_e \right) = -en_e u_e \cdot E - n_e v_{ion} \phi E_i - S_{wall} \quad (4)$$

Ion moves directly by electrostatic force, and Rarmor motion of ion is neglected.

On the channel surface, an electric sheath as shown in Figure.9 is produced. The sheath length is assumed to be six times the Debye length; that is, is six as follows:

$$d_s = a\lambda_D \quad \lambda_D = \left(\frac{\epsilon_0 kT_e}{n_e e^2} \right)^{1/2} \quad (5)$$

The secondary electron emission coefficient of channel insulator is written as follows:

$$\delta_{eff} = \Gamma[2+B] A \left(\frac{kT_e}{e} \right)^B \quad (6)$$

where Γ is Gamma function, and A and B are constants depending on insulator material species. The constants of boron nitride were assumed to be A=0.141 and B=0.576. Accordingly, the wall potential is determined as follows:⁷

$$\phi_w = -\frac{kT_e}{e} \left[\frac{1}{2} + \ln \left\{ \left(\frac{\bar{C}_e}{4V_b} \right) (1 - \delta_{eff}) \right\} \right] \quad (\delta_{eff} < 1)$$

$$\phi_w = T_{sec} \ln \delta_{eff} \quad (\delta_{eff} > 1) \quad (7)$$

where the secondary emission electron temperature T_{sec} is assumed to be 0.5 eV.

The neutral particle temperature is assumed to be 1000 K at the upstream end in the acceleration channel, and the electron temperature is 5.0 eV at the downstream boundary in the calculation domain; that is, the electron emitted from the hollow cathode has 5.0 eV of temperature.

The channel surface is shaved by ion sputtering; that is, the surface moves backward. In this calculation, the calculation domain, as shown in Figure.8, includes the channel insulator, and therefore the movement of the surface can be simulated. The movement of mesh grids is shown in Figure.10. The amount of sputtered insulator particles depends on flux, energy and direction of bombarding ions. We used the data of sputtering of Xe ion against BN in Ref. 10 as shown in Figure.11 and Table 3.

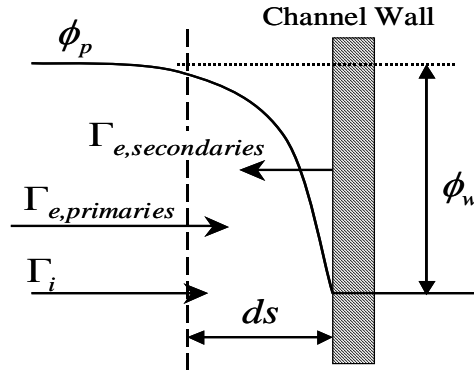


Figure 9. Features of sheath on the channel wall.

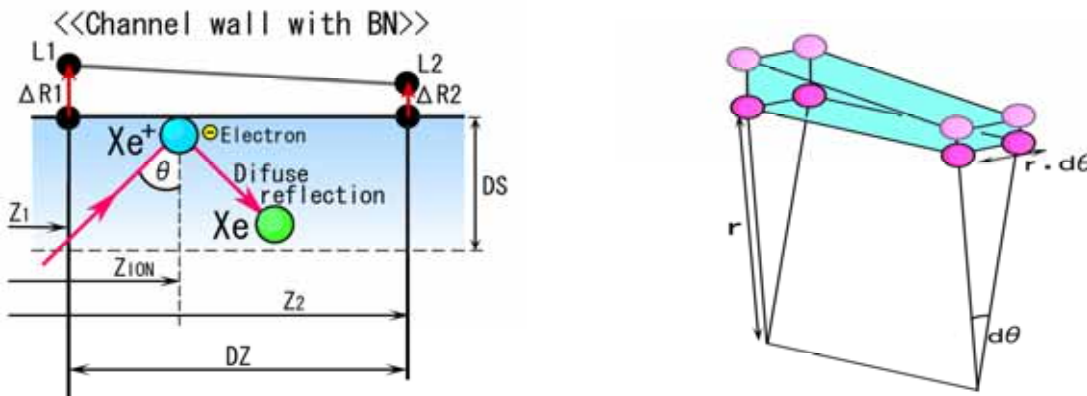
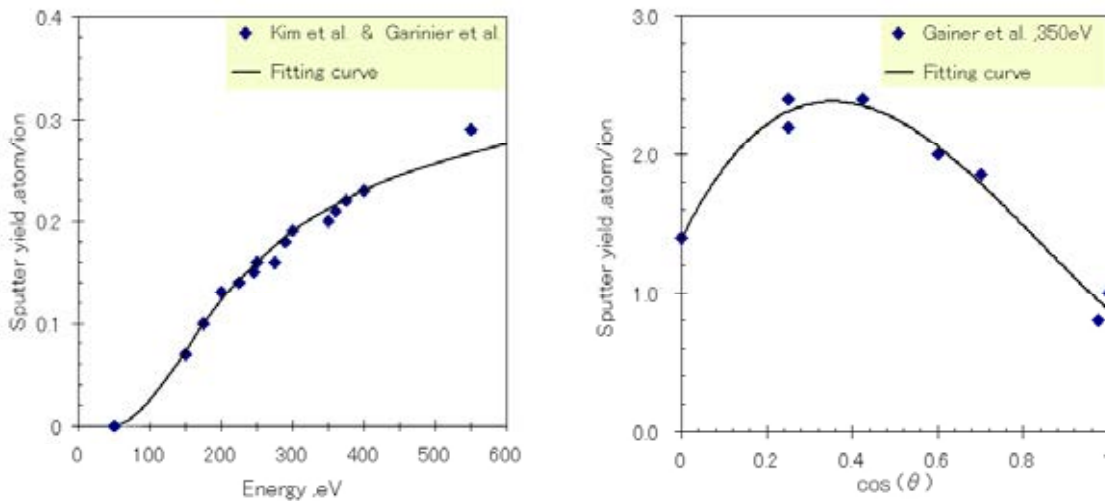


Figure 10. Movement of mesh grids for calculation.



(a) Dependence of ion energy.

(b) Dependence of ion impact angle.

Figure 11. Sputtering yield for Xe ion on BN.

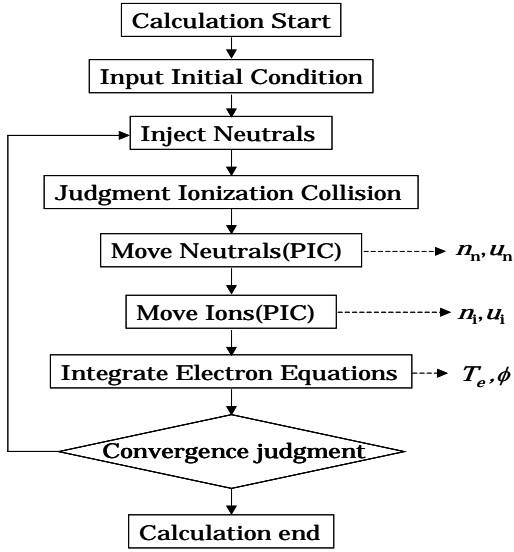


Figure 12. Flowchart for calculation.

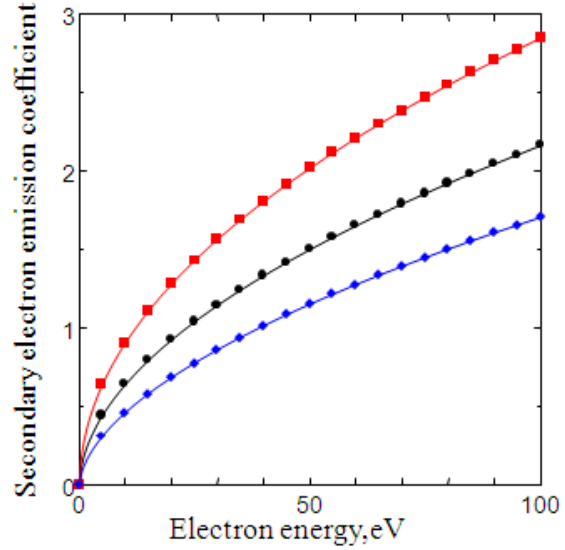


Figure 13. The secondary electron emission coefficients

Table 3. Boron nitride properties.

Grade	N-1
Density	1.8 [g/cm ³]
Hardness	12 [shorr]
Flexural strength	30 [MPa]
Heat conductivity	63 [W/mK]
Maximum operation temperature	In atmosphere 950[°C] In inertgas 2200[°C] In vacuum 2000[°C]
Dielectric constant	4.5 [MHz,RT]
Dielectric loss	0.9 [tan δ × 10 ⁻³ (1MHz,RT)]
Volume resistance	10 ¹³ [Ω cm]
Chemical structure	99 or more [%]
Other components	-

IV. Experimental Results and Discussion

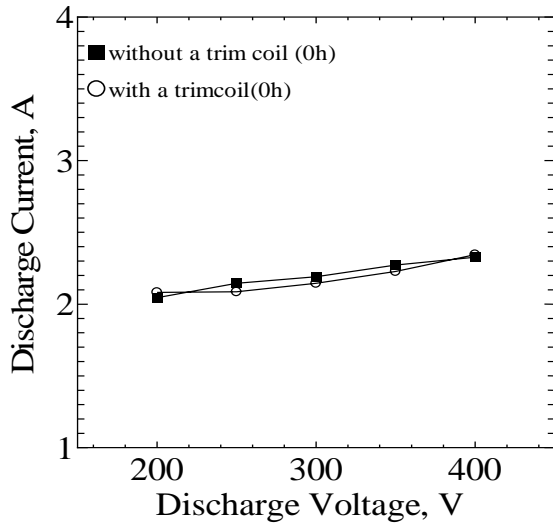
Performance characteristics were evaluated over discharge voltages of 200-400 V at a constant mass flow rate of 2 mg/s with cases with and without the trim coil and cases with changing acceleration channel geometry.

A. Influence of Trim coil on performance

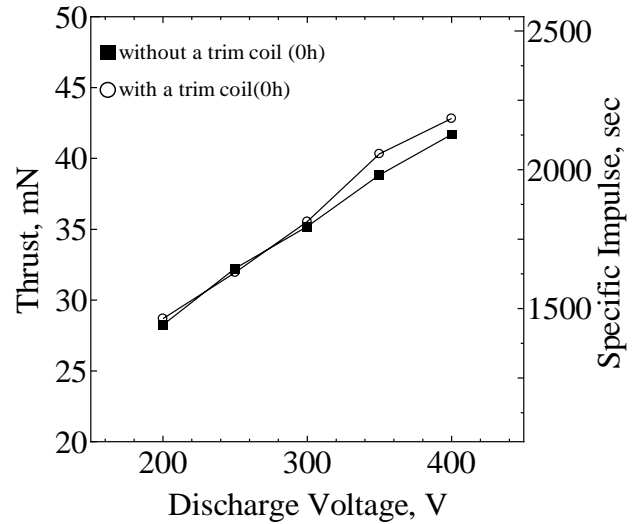
Figure 14 shows the discharge current vs voltage characteristics with and without the trim coil. At a fixed voltage, the discharge current slightly decreases when the trim coil is energized. This reason might be considered as follows. A trim coil reduces the magnetic field near the anode, and increases the value of γ_{se} . Electrons stay less time in the channel by the lower magnetic field near the anode, which leads to moderate electron heating in the anode region

and to prevent excessive ionization. Smaller amount of electrons flowing into the anode led to lower discharge current.

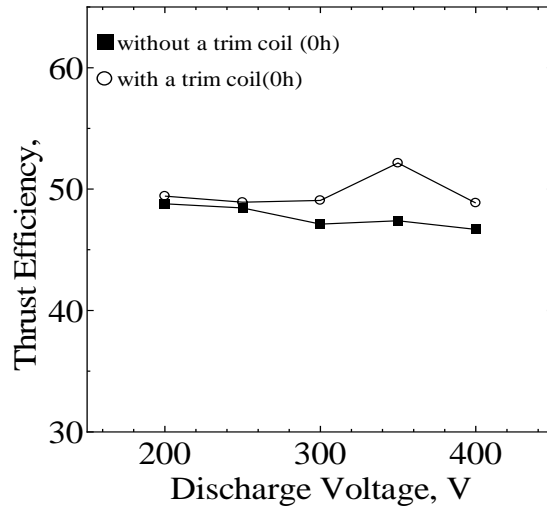
As shown in Figure.14(b), the trim coil increases thrust in the high voltage region above 300 V. This is expected because the ionization region is pushed toward downstream when the region of large magnetic field moves toward the channel exit with the trim coil. This shift moderates ion losses to the channel walls, and ions are efficiently extracted from the thruster. Accordingly, the thrust efficiency, as shown in Figure.14(c), is enhanced at high discharge voltages above 300 V.



(a) Discharge current.



(b) Thrust and specific impulse.



(c) Thrust efficiency.

Figure 14. Performance characteristics with and without trim coil.

B. Influences of channel geometry; prediction of performance change in long operations

Figure 15 shows plasma exhaust plume features at a discharge voltage of 300 V for predicted operational times of 0-300 hours. The plasma plume feature is observed to intensively change as the operational time increases. With 200 and 300 h an intensive jet on the axis disappears, and radial expansion is relatively large near the outer channel exit.

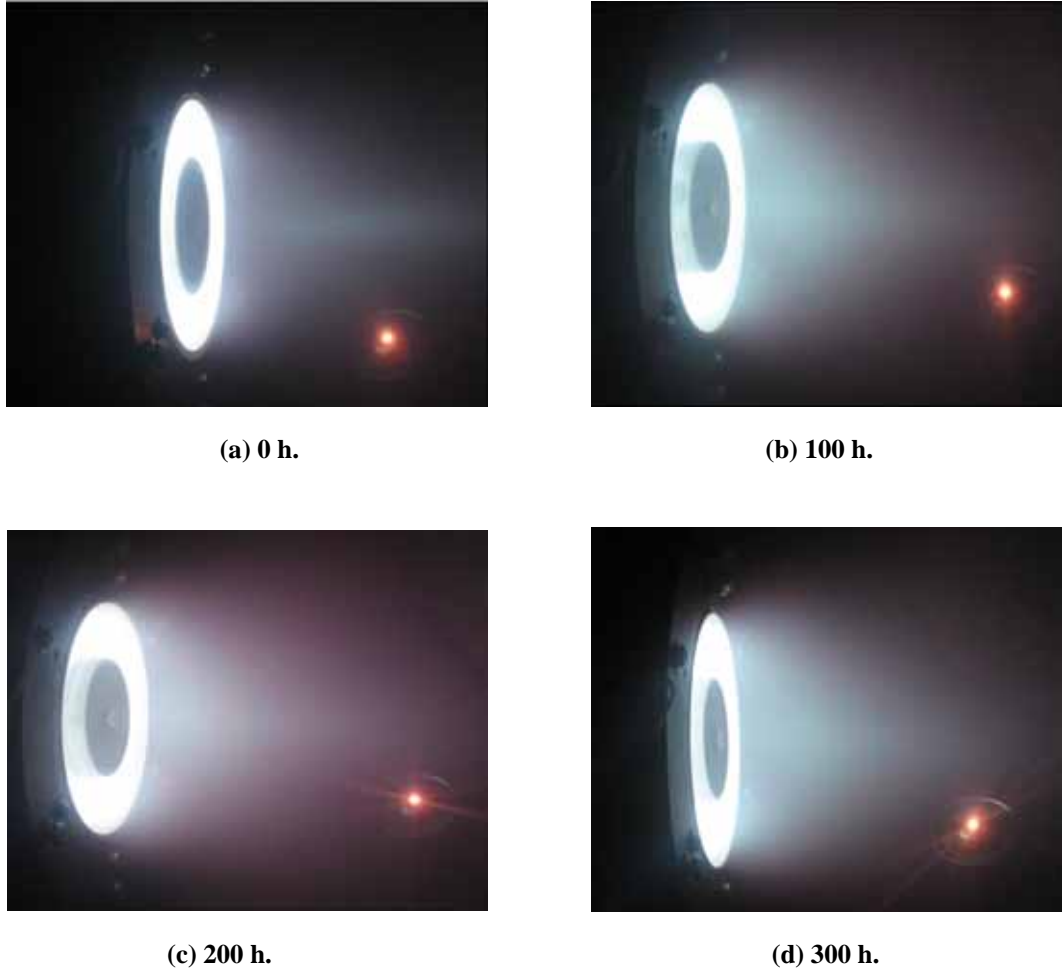
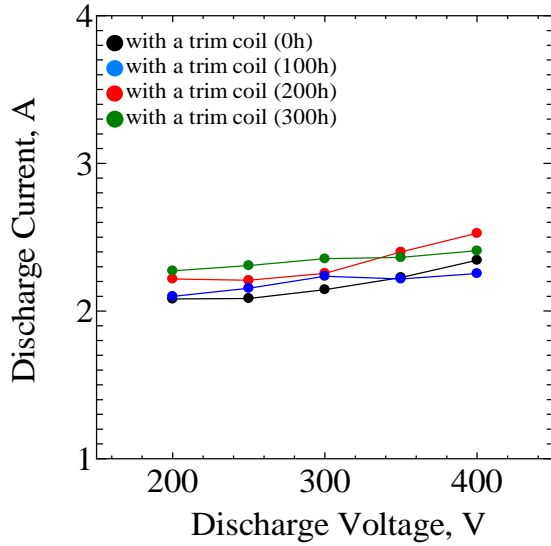


Figure 15. Plasma exhaust plume features at 300 V.

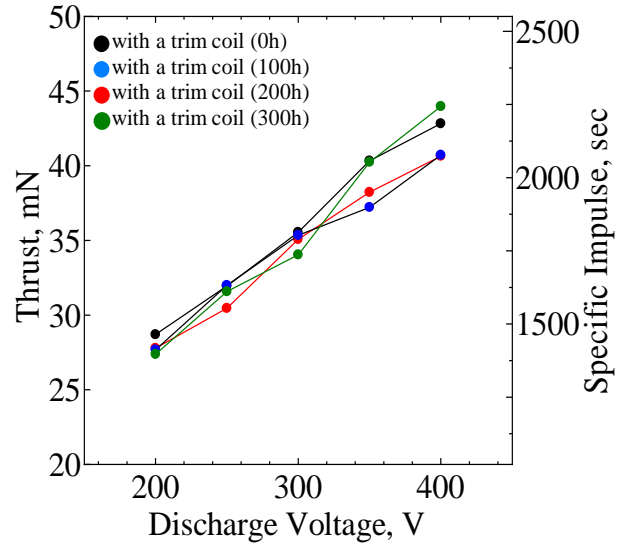
Figure 16 shows the performance characteristics with the trim coil. The performance with the trim coil qualitatively agreed with that without the trim coil. The discharge current roughly seems to increase with increasing predicted operational time up to 200 h, that is, with shaving channel wall, at a constant discharge voltage, although with the highest predicted time of 300 h it becomes lower. The thrust decreases with an increase in predicted operational time except for cases with discharge voltages of 350 and 400 V at 300 h. The thrust at 300 h is higher than that at 0 h with 350 and 400 V. As a result, the thrust efficiency roughly decreases with increasing predicted operational time at constant discharge voltages below 300 V. However, with 350 and 400 V the thrust efficiency intensively becomes higher. These phenomena are expected because the ionization and acceleration regions move upstream near the acceleration channel exit by enlarging channel volume and cross-section, resulting in enhancement of ion losses on the channel walls, with low predicted times of 100 and 200 h, and because smooth plasma expansion through magnetic field lines is achieved with 300 h although radial expansion, resulting in decreasing thrust, is slightly enhanced.

Figure 17 shows the discharge current oscillations with the trim coil. The oscillation frequency of discharge current is about 12 kHz with all operational conditions. The oscillation amplitude intensively increases with

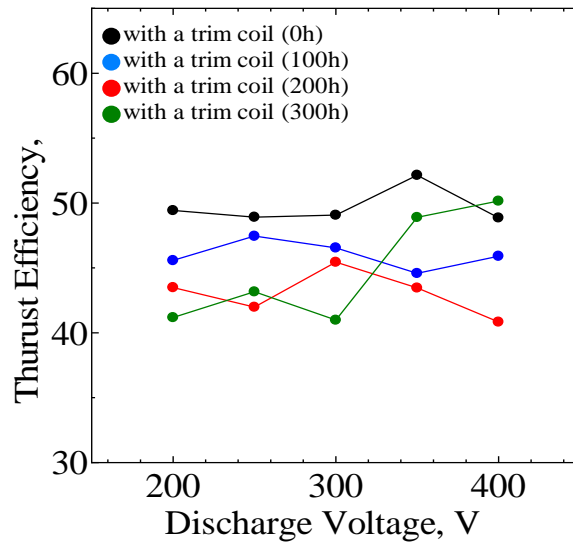
increasing predicted operational time at a constant discharge voltage. The characteristics of discharge current oscillation agreed with discharge observation with the high speed camera. Accordingly, operational stability becomes low with increasing predicted operational time, i.e., with shaving channel wall.



(a) Discharge current.



(b) Thrust and specific impulse.



(c) Thrust efficiency.

Figure 16. Performance characteristics with trim coil for predicted operational times of 0-300 h.

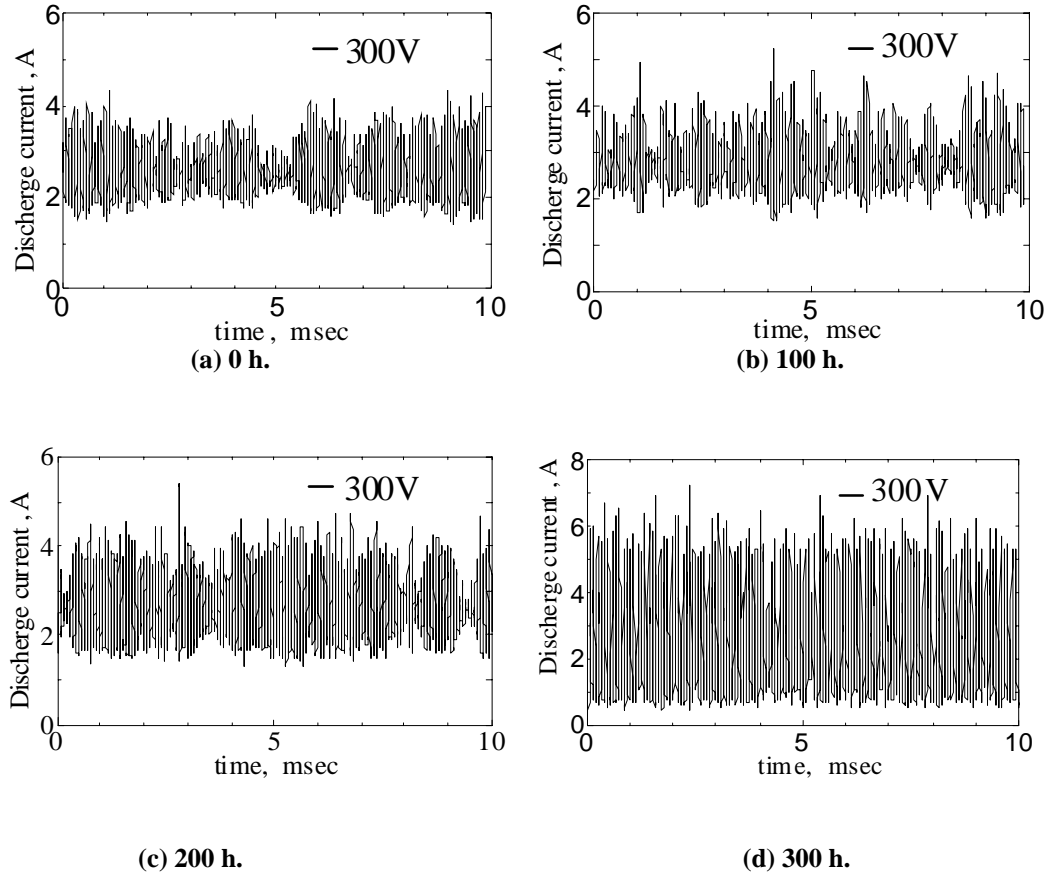


Figure 17. Discharge current oscillations with trim coil for predicted operational times of 0-300 h.

V. Calculated Results and Discussion

A. Calculated performance characteristics

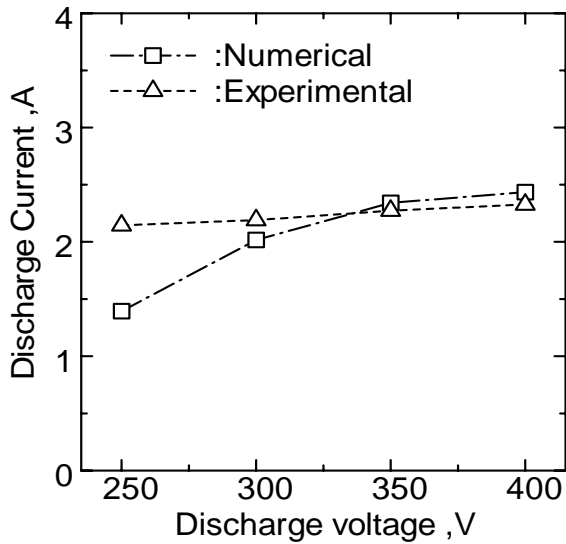
Figure 18 shows the calculated performance characteristics with the trim coil and a straight BN acceleration channel, i.e., an operational time of zero, at discharge voltages of 250-400 V. Both the calculated discharge current and the calculated thrust increase with increasing discharge voltage as well as the measured ones shown in Figure.16(a). However, the rates of increase for the calculated ones are higher than those for the measured ones, although the values quantitatively agree with the measured ones except for a case with the lowest discharge voltage of 250 V. This is expected because with 250 V the ionization degree for the calculation is smaller than that for the experiment, resulting from a simplified ionization model with only direct collisional ionization between electron and Xe atom in the calculation. As a result, the calculated thrust efficiency also agrees well with the measured one except for the case with 250 V.

B. Calculated inner plasma features

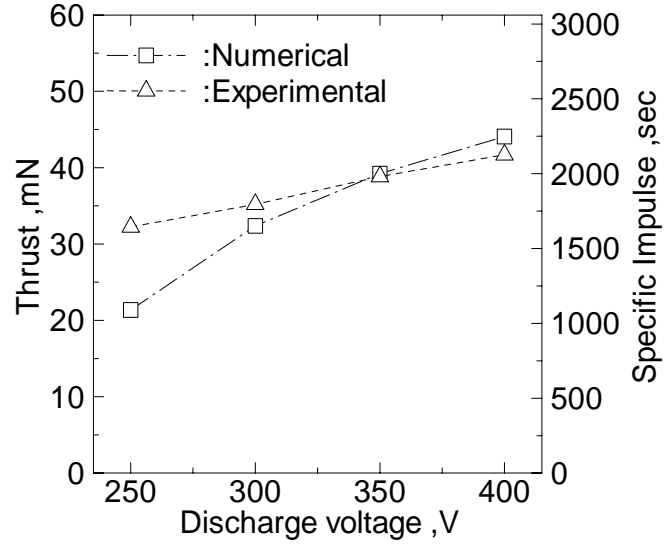
Figure 19 shows the calculated spatial distributions of plasma properties with the trim coil at a discharge voltage of 400 V. The plasma potential slowly goes down from the upstream end, i.e., from the anode, to about 20 mm in the BN acceleration channel, and from 20 mm to the downstream boundary it intensively decreases. The potential drop near the channel walls results from both effects of secondary electron emission and recombination.

The electron temperature, as shown in Figure.19(b), has a peak between 20 and 30 mm in the acceleration channel, and from the peak to the downstream end it intensively decreases. Therefore, electrons emitted from the hollow

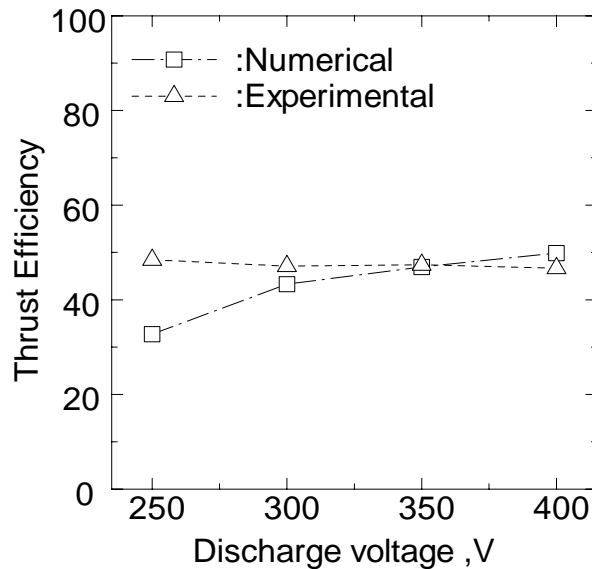
cathode are accelerated in the upstream direction; intensive ionization collisions are induced with the energized electrons from 20-30 mm to the anode, and produced ions are drastically accelerated in the downstream direction with the large potential drop from 20 mm to the downstream boundary. The ion number density, as shown in Figure.19(c), agrees with these phenomena. The ion density is also found to be very low near the channel walls because of recombination.



(a) Discharge current.

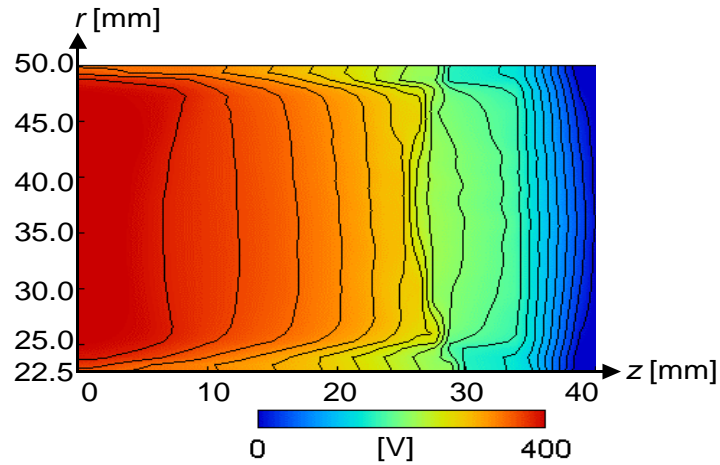


(b) Thrust and specific impulse.

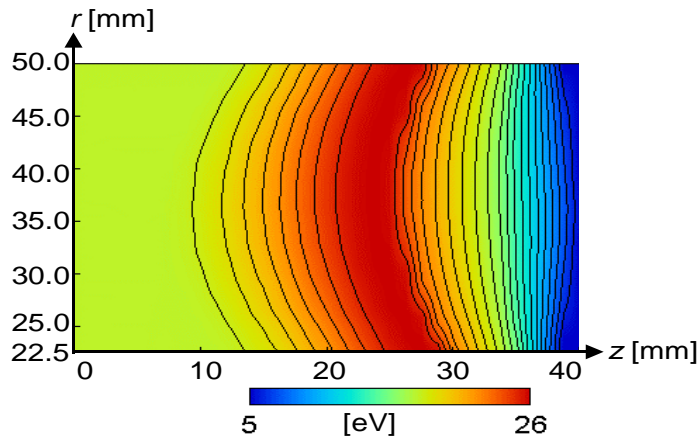


(c) Thrust efficiency.

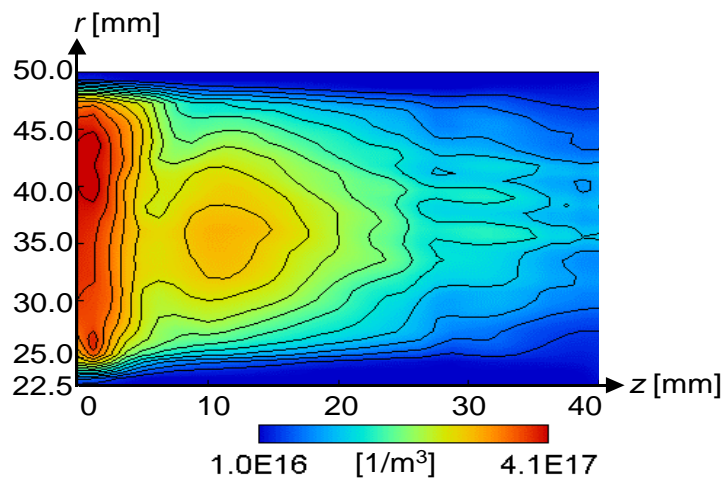
Figure 18. Calculated performance characteristics with trim coil for predicted operational time of 0 h.



(a) Plasma potential.



(b) Electron temperature.

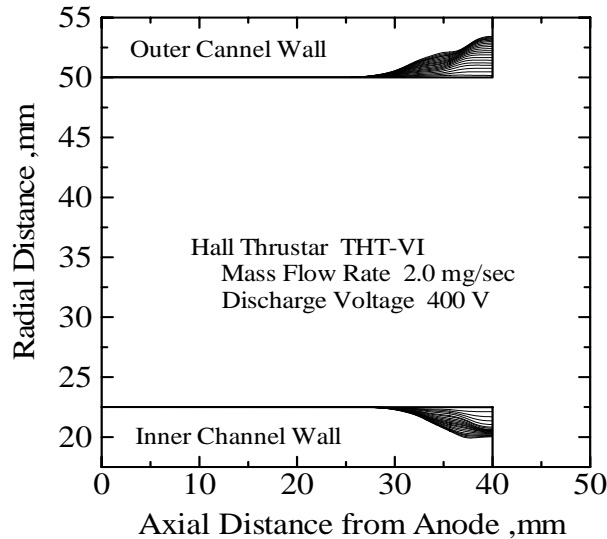


(c) Ion number density.

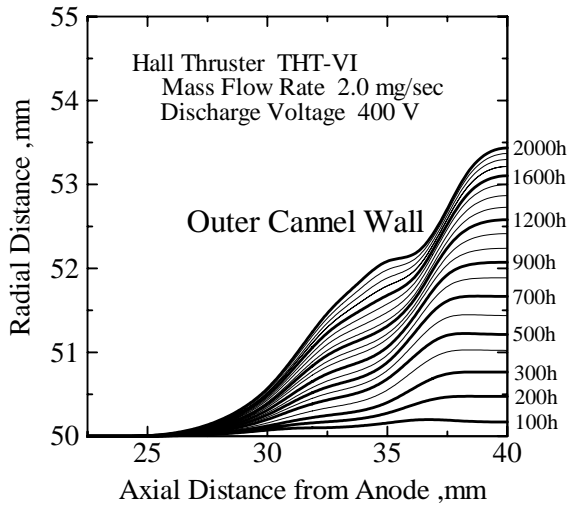
Figure 19. Calculated spatial distributions of plasma physical properties in acceleration channel with trim coil at 400 V with 0 h.

C. Calculated change of channel geometry in long operations.

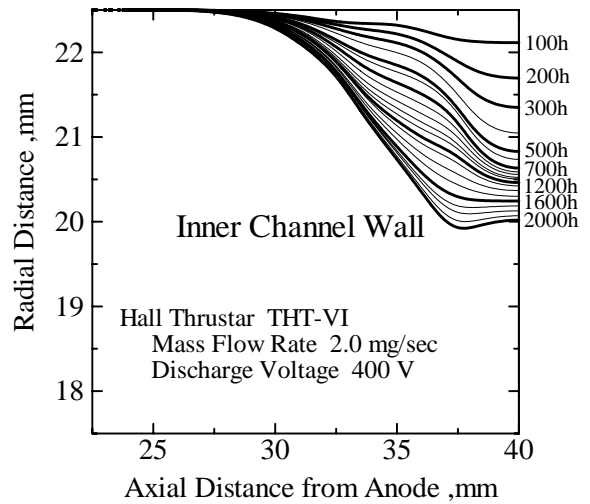
Figure 20 shows the calculated variations of channel geometry during an operational time of 2000 h at a discharge voltage of 400 V. The BN acceleration channel is intensively shaved near the downstream exit by spattering enhanced with highly accelerated ions. The shaved depths of the inner and outer channel walls are about 1 mm with 250 and 400 h, respectively; that is, the inner channel wall is relatively severe compared with the outer channel wall. When compared with the experimental channel geometries used in this study as shown in Figure.6, the experimental shaved values are about three times the calculated ones at the same operational time. Consequently, more study is needed considering both experiment and calculation.



(a) Overview of channel walls.



(b) Outer channel wall.



(c) Inner channel wall.

Figure 20. Calculated variations of channel geometry during operational time of 2000 h at 400 V with trim coil.

D Dependence of channel material species on performance and plasma feature

Figure 21 shows the calculated spatial distributions of electron temperature with Al_2O_3 , BN and BNAIN channels at 400 V. The electron temperature with Al_2O_3 is intensively low compared with those with BN and BNAIN although with BNAIN it is very high. This is because of cooling effect enhanced with the highest secondary electron coefficient of Al_2O_3 although with BNAIN intensive ionization occurs with high energy electrons. As shown in Figure.22, the surface potential on the inner channel wall with Al_2O_3 is the smallest on the plasma potential, although with BNAIN it is very large resulting in severe ion sputtering.

The calculated discharge currents and thrusts were 1.78 A and 33.7 mN with Al_2O_3 , 1.96 A and 35.3 mN with BN and 2.46 A and 44.9 mN with BNAIN. The BNAIN channel shows the highest performance.

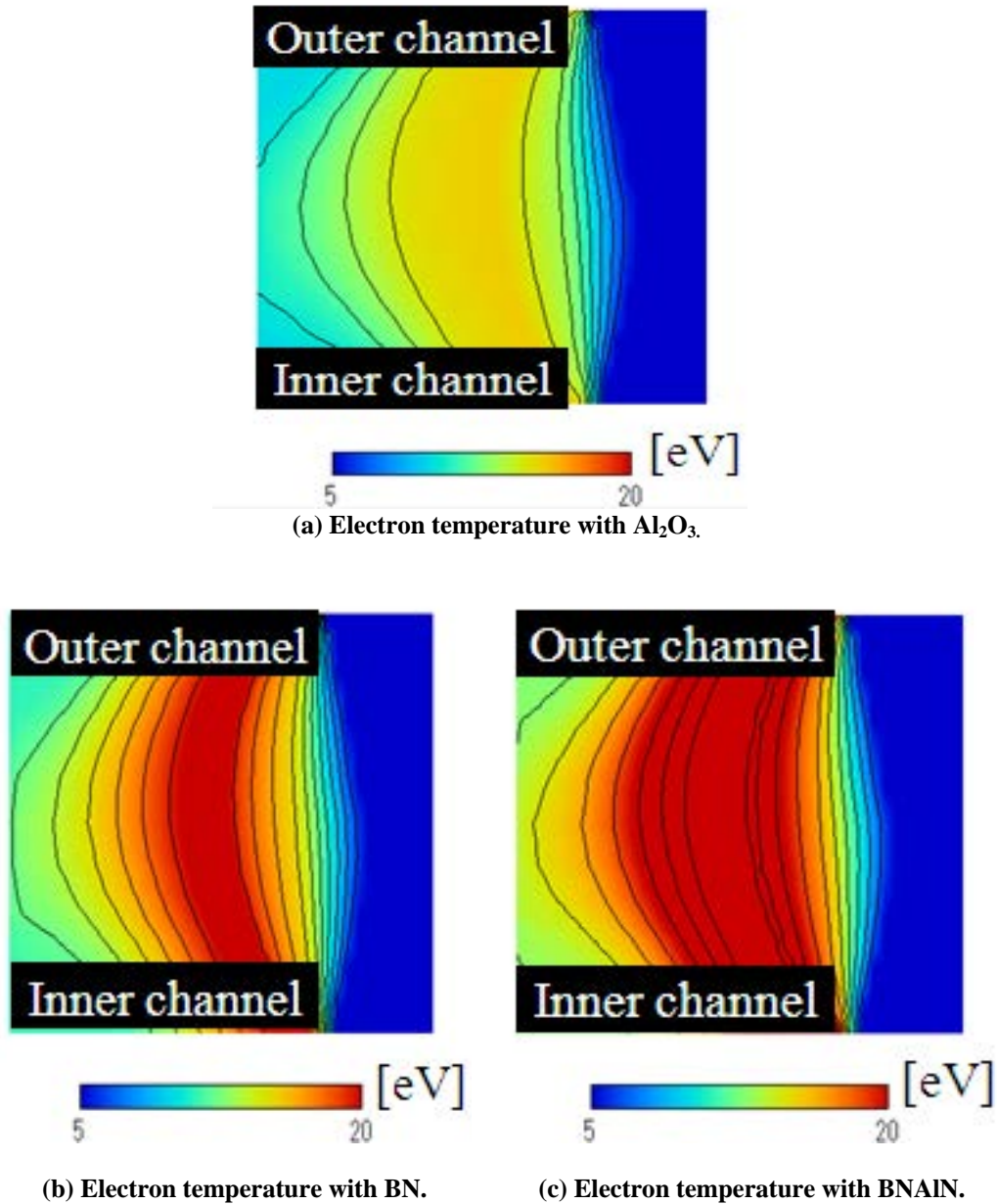


Figure 21. Calculated spatial distributions of electron temperature with Al_2O_3 , BN and BNAIN channels at 400 V.

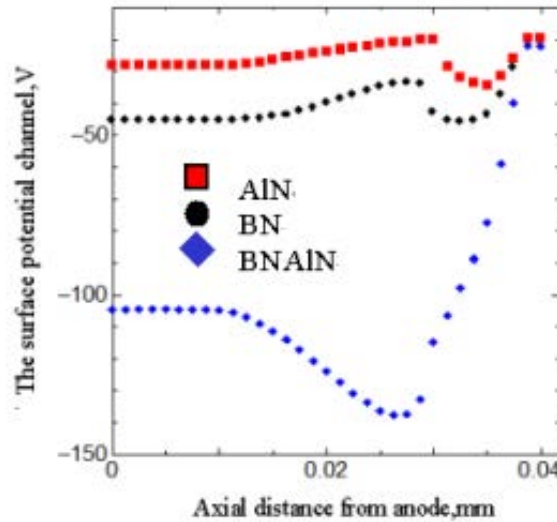


Figure 22. Surface potential on inner channel wall with Al_2O_3 , BN and BNAIN.

VI. Conclusions

To study influences of magnetic topology on performance and influences of channel geometry, i.e., prediction of performance change during long operations, a laboratory model THT-VI thruster with a trim coil was operated at discharge voltages of 200-400 V and a xenon mass flow rate of 2.0 g/s. The THT-VI Hall thruster has the same acceleration channel as Russian SPT100 Hall thruster.

At a fixed voltage, the discharge current slightly decreased when the trim coil was energized. The trim coil increased thrust in the high voltage region above 300 V. Accordingly, the thrust efficiency was enhanced at the high discharge voltages.

The BN acceleration channel structure was modified to examine influences of channel geometry. Particularly, to predict changes of performance characteristics during long operations, near-exit regions of the channel walls were shaved. The plasma plume feature was observed to intensively change as the predicted operational time increased. With 200 and 300 h an intensive jet on the axis disappeared, and radial expansion was relatively large near the outer channel exit. The discharge current roughly increased with increasing predicted operational time up to 200 h, although with the highest predicted time of 300 h it became lower. The thrust decreased with an increase in predicted operational time except for cases with discharge voltages of 350 and 400 V at 300 h. The thrust at 300 h was higher than that at 0 h with 350 and 400 V. As a result, the thrust efficiency roughly decreased with increasing predicted operational time at constant discharge voltages below 300 V. However, with 350 and 400 V the thrust efficiency intensively became higher. These phenomena are expected because the ionization and acceleration regions move upstream near the acceleration channel exit by enlarging channel volume and cross-section. The oscillation frequency of discharge current was about 12 kHz with all operational conditions. The oscillation amplitude intensively increased with increasing predicted operational time. Accordingly, operational stability became low with increasing predicted operational time.

Numerical calculation was carried out by means of hybrid PIC method. Both the calculated discharge current and the calculated thrust increased with increasing discharge voltage as well as the measured ones. However, the rates of increase for the calculated ones were higher than those for the measured ones, although the values quantitatively agreed with the measured ones except for a case with the lowest discharge voltage of 250 V. This is expected because with 250 V the ionization degree for the calculation is smaller than that for the experiment. As a result, the calculated thrust efficiency agreed well with the measured one except for the case with 250 V.

With a discharge voltage of 400 V, the calculated plasma potential slowly went down from the upstream end, i.e., from the anode, to about 20 mm in the BN acceleration channel, and from 20 mm to the downstream boundary it intensively decreased. The electron temperature had a peak between 20 and 30 mm in the acceleration channel, and

from the peak to the downstream end it intensively decreased. Therefore, electrons emitted from the hollow cathode are accelerated in the upstream direction; intensive ionization collisions are induced with the energized electrons from 20-30 mm to the anode, and produced ions are drastically accelerated in the downstream direction with the large potential drop from 20 mm to the downstream boundary.

With a discharge voltage of 400 V, the acceleration channel was intensively shaved near the downstream exit by spattering enhanced with highly accelerated ions. The shaved depths of the inner and outer channel walls were about 1 mm with 250 and 400 h, respectively; that is, the inner channel wall was relatively severe compared with the outer channel wall. When compared with the experimental channel geometries used in this study, the experimental shaved values were about three times the calculated ones at the same operational time.

Furthermore, we estimated the dependence of channel material species by changing secondary electron emission coefficient. The calculated electron temperature with Al_2O_3 was intensively low compared with those with BN and BNAIN although with BNAIN it was very high. This is because of cooling effect enhanced with the highest secondary electron coefficient of Al_2O_3 although with BNAIN intensive ionization occurred with high energy electrons. The calculated surface potential on the inner channel wall with Al_2O_3 was the smallest on the plasma potential, although with BNAIN it was very large resulting in severe ion sputtering. The calculated discharge currents and thrusts were 1.78 A and 33.7 mN with Al_2O_3 , 1.96 A and 35.3 mN with BN and 2.46 A and 44.9 mN with BNAIN. The BNAIN channel showed the highest performance.

References

- ¹ Britt, E. and McVey, J.: Flow Periodicity Improvement in a High Speed Compressor Cascade with a Large Turning-Angle, in *proceedings of the 38th AIAA Joint Propulsion Conference, Indianapolis, Indiana (American Institute of Aeronautics and Astronautics, Reston, VA, 2002)*, AIAA Paper 2002-3559, 2002.
- ² Yuge, S. and Tahara, H.: Performance Enhancement of a 1-kW Anode-layer Hall Thruster, 29th International Electric Propulsion Conference, Princeton, IEPC Paper 2005-020, 2005.
- ³ Imanaka, K., Shirasaki, A., Yuge, S. and Tahara, H.: Effect of Channel Wall Material on Hall Thruster Performance, 24th International Symposium on Space Technology and Science, Miyazaki, ISTS Paper 2004-b-30, 2004.
- ⁴ Tahara, H., Yuge, S., Shirasaki, A. and Martinez-Sanchez, M.: Performance Prediction of Hall Thrusters Using One-Dimensional Flowfield Calculation, 24th International Symposium on Space Technology and Science, Miyazaki, ISTS Paper 2004-b-53p, 2004.
- ⁵ Tahara, H., Shirasaki, A., Yuge, S. and Yosikawa, T.: Optimization of Magnetic Field and Acceleration Channel for Low Power Hall Thrusters, 24th International Symposium on Space Technology and Science, Miyazaki, ISTS Paper 2004-b-54p, 2004.
- ⁶ Kim, V.: Main Physical Futures and Processes Determining the Performance of Stationary of a Hall Thrusters, *Journal of Propulsion and Power*, Vol.14, No.5, 1998, pp.736-743.
- ⁷ Gavryushinn, V.M., Kim, V., Kozlov, V.I. and Maslennikov, N.A.: Physical and Technical Bases of the Modern SPT Development, in *Proceedings of the 24th International Electric Propulsion Conference, Moscow, Russia (Electric Rocket Propulsion Society, Cleveland, OH, 1995)*, IEPC Paper 95-38, 1995.
- ⁸ Parra, F.I. and Ahedo, E., Fife, J.M. and Martinez-Sanchez, M.: A Two-Dimensional Hybrid Model of the Hall Thruster Discharge, *J. Appl. Phys.*, Vol.100, 023304, 2006.
- ⁹ Yim, J.T., Keider, M. and Boy, I.D.: A Hydrodynamic-Based Erosion Model for Hall Thrusters, 25th International Electric Propulsion Conference, IEPC Paper 2005-013, 2005.
- ¹⁰ Mathur, D. and Badrinathan, C.: Ionization of Xenon by Electron: Particle Cross Section for Single, Double and Triple Ionization, *Physical Review A*, Vol.35, No.3, 1987, pp.1033-1042.